

Evidence for Clean d-wave Superconductivity in Samarium Nickelates

Qingming Huang^{†1}, Xiaofang Fu^{†2,3}, Junlong Wu^{†2,3}, Laifeng Li^{*4}, Liang Qiao^{*2,3} and Ye Yang^{*1}

1. The State Key Laboratory of Physical Chemistry of Solid Surfaces, College of Chemistry & Chemical Engineering, Xiamen University, Xiamen 361005, China
2. School of Physics, University of Electronic Science and Technology of China, Chengdu, 611731, China
3. State Key Laboratory of Electronic Thin Films and Integrated Devices, University of Electronic Science and Technology of China, Chengdu 611731, China
4. State Key Laboratory of Cryogenic Science and Technology, Technical Institute of Physics and Chemistry, Chinese Academy of Sciences, Beijing 100190, China

† These authors contributed equally.

* lqli@mail.ipc.ac.cn; liang.qiao@uestc.edu.cn; ye.yang@xmu.edu.cn

Abstract: The discovery of superconducting nickelates provides a unique opportunity to explore the pairing mechanism of high-temperature superconductivity. Here, we use ultrafast terahertz spectroscopy to probe the temperature-dependent superfluid density in an infinite-layer samarium nickelate film with a T_c of 20 K. The superfluid density decreases linearly with rising temperature, consistent with clean limit d-wave pairing. From this linear relation, we extract a superconducting gap $\Delta(0) = 2.5 \pm 0.1$ meV and a gap-to- T_c ratio, $2\Delta(0) / k_B T_c \approx 3$, suggesting that this sample lies in the weak-coupling limit. Furthermore, the ratio of mean free path to coherence length, l/ξ , is determined to be 1.5, confirming the clean-limit behavior. These findings establish strong parallels between the pairing mechanisms in nickelate and cuprate superconductors.

The discovery of superconductivity in infinite-layer nickelates has spurred intense research into their similarities with and distinctions from high-temperature cuprate superconductors.[1] One of the most important and enduring problems in these superconductors concerns the pairing mechanism, which is the key to understanding the nature and origin of the high-temperature superconductivity. Although nickelates share similar crystal and electronic structures with cuprates, critical questions regarding the electron pairing symmetry remain unsolved. Many theoretical

studies on pairing instability predict a dominant $d_{x^2-y^2}$ pairing symmetry in the nickelate superconductors, analogous to cuprates, while others propose multiorbital nature.[2-9] Meanwhile, the experimental results provide a complex picture for the pairing symmetry. Scanning tunneling spectroscopy has revealed distinct gap structures consistent with both s-wave and d-wave pairing.[10] Temperature-dependent measurement of London penetration depth in different rare-earth nickelate films indicates both nodal d-wave and nodeless multigap pairing.[11,12] A recent terahertz (THz) spectroscopic study on a Sr-doped neodymium nickelate film suggests d-wave superconductivity in the dirty limit.[13]

Due to current synthetic limitations, surface-sensitive techniques like angle-resolved photoemission spectroscopy face challenges in probing the superconducting state of the infinite-layer nickelates.[10,14,15] In contrast, bulk-sensitive techniques like THz spectroscopy are less hindered by these limitations.[11-13] The intriguing yet inconsistent results mentioned above underscore the need to clarify the pairing symmetry across the nickelate family. The recent achievement of significantly enhanced superconductivity in samarium nickelate films[16,17] renders them a particularly compelling system for such a study. However, the low superfluid density of nickelate superconductors poses a challenge for equilibrium THz spectroscopy because the equilibrium THz response is dominated by the normal fluid (i.e., thermal quasiparticles) even at temperatures well below T_c ,[13] and then the superfluid signature can be easily overwhelmed, particularly at elevated temperatures. In contrast, the transient THz response selectively probes the conductivity change arising from the photo-destroyed superfluid, with negligible contribution from the equilibrium normal fluid.[13,18] This selectivity makes transient THz spectroscopy a precise tool for examining the superfluid response across a wide temperature range.

Here, we employ time-resolved optical pump-THz probe spectroscopy to investigate the photoinduced conductivity and photogenerated quasiparticle dynamics in a superconducting samarium nickelate film. The transient complex conductivity uncovers a photoinduced spectral weight transfer from superfluid to Drude response after optical excitation, a hallmark of Cooper pair breaking and quasiparticle formation. The recovery kinetics of the THz response are governed by bimolecular recombination of the photogenerated quasiparticles. Crucially, temperature-dependent measurements show a linear decreasing trend of the photo-destroyed superfluid density with rising temperature, consistent with the clean d-wave pairing. The ratios of the gap to T_c and the mean free path to the coherence length, derived from the experimental results, provide evidence for weak-coupling superconductivity with d-wave pairing symmetry in the clean limit.

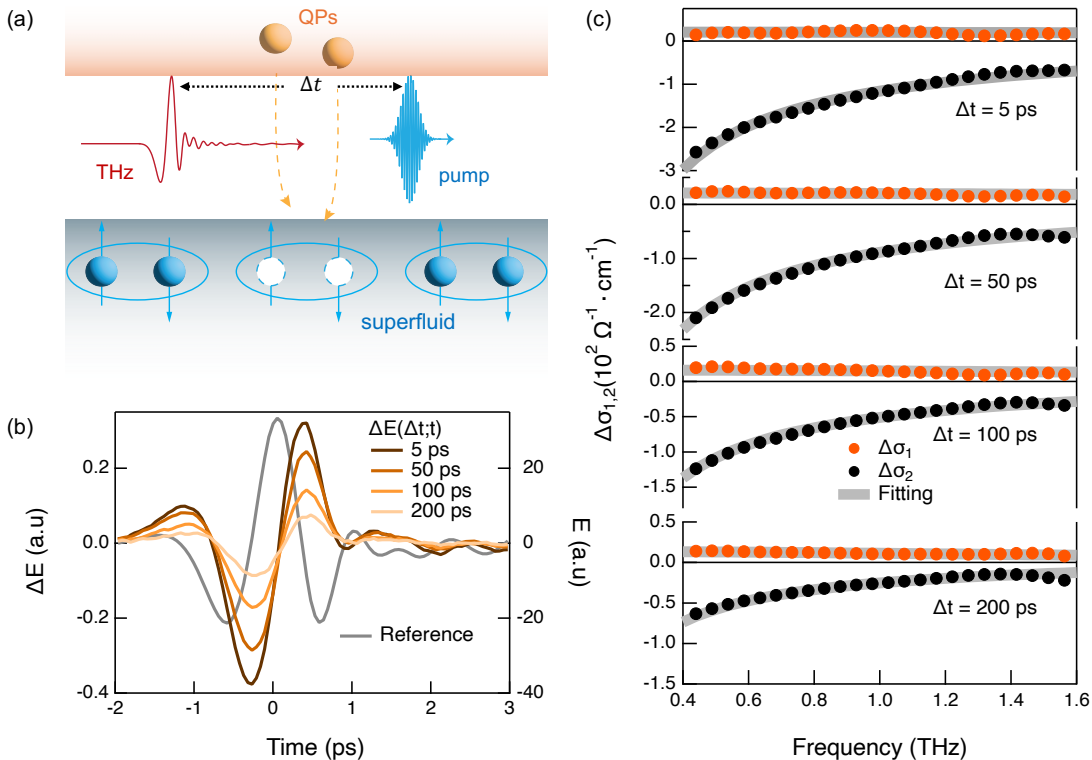


Figure 1. Photoinduced THz conductivity change of nickelate SC films at 3 K. (a) Schematic illustration optical excitation of condensed Cooper pairs. (b) Comparison between the reference

THz waveform, $E(t)$, and signal waveforms, $\Delta E(t; \Delta t)$, recorded at representative pump-THz delays (Δt). (c) Real ($\Delta\sigma_1$, orange dots) and imaginary ($\Delta\sigma_2$, black dots) parts of the photoinduced change of the complex conductivity at indicated Δt . The gray dash curves represent the fitting curves based on the two-fluid model.

The $\text{Sm}_{0.75}\text{Ca}_{0.05}\text{Eu}_{0.2}\text{NiO}_2$ thin film with a thickness of 10 nm was epitaxially grown on a $(\text{La},\text{Sr})(\text{Al},\text{Ta})\text{O}_3$ (LSAT) substrate via pulsed laser deposition.[19] The electrical resistance of this nickelate film drops to zero at 20 K (Fig. S1), which is regarded as T_c . In the optical pump-THz probe measurements, a pump pulse ($h\nu=1.55$ eV) drives the superconducting nickelate film out of equilibrium, and a subsequent THz probe pulse measures the recovery process (Fig. 1a). The time delay (Δt) between pump and probe pulses was controlled by an optical delay line. additional experimental details are provided in Supplementary Material. The transmitted THz electric field in the time domain, $E(t)$, where t is the time delay between the THz generation and detection pulses, is recorded as a reference. As shown in Fig. 1b, the photoinduced change in this field, $\Delta E(t; \Delta t)$, show a significant temporal shift compared to $E(t)$. As Δt increases, the amplitude of $\Delta E(t; \Delta t)$ decays progressively, whereas the shape of $\Delta E(t; \Delta t)$ remains unchanged, which indicates a clean recovery process without the formation of other transient species.

The frequency-dependent transient complex conductivity ($\Delta\tilde{\sigma}$) is extracted from the ratio of $\Delta\tilde{E}(\omega; \Delta t)/\tilde{E}(\omega)$, where $\Delta\tilde{E}(\omega; \Delta t)$ and $\tilde{E}(\omega)$ are the Fourier transforms of $\Delta E(t; \Delta t)$ and $E(t)$, respectively. At $T = 3$ K, $\Delta\tilde{\sigma}$ displays a positive, Drude-like real part ($\Delta\sigma_1$) and a negative imaginary part ($\Delta\sigma_2$) that follows a $1/\omega$ dependence. This spectral signature indicates a photoinduced spectral weight transfer from the superfluid response to the Drude response, a hallmark of Cooper pair breaking and concurrent formation of quasiparticles, as previously observed in both nickelate and cuprate superconductors.[13,18,20-22] The $\Delta\tilde{\sigma}$ spectra for different

Δt are well described by a phenomenological two-fluid model (grey curves, Fig. 1c),[13,18] expressed as

$$\Delta\tilde{\sigma}(\omega) = i \frac{\Delta\rho_s}{\omega} + \frac{\Delta\rho_n}{\tau_n^{-1} - i\omega} \quad (1)$$

where $\Delta\rho_s$ and $\Delta\rho_n$ are the effective densities of broken Cooper pairs and the resulting quasiparticles, respectively, and τ_n^{-1} is the scattering rate of those photogenerated quasiparticles. In accordance with the spectral weight conservation, $\Delta\rho_n = -\Delta\rho_s$. As Δt increases, both $\Delta\sigma_1$ and $\Delta\sigma_2$ exhibit a concurrent decay, reflecting the recovery of the superfluid density via the re-pairing of photogenerated quasiparticles. Throughout this study, the pump fluence was maintained sufficiently low to guarantee a linear relationship between the amplitude of $\Delta\tilde{\sigma}$ and the pump fluence (Fig. S2).

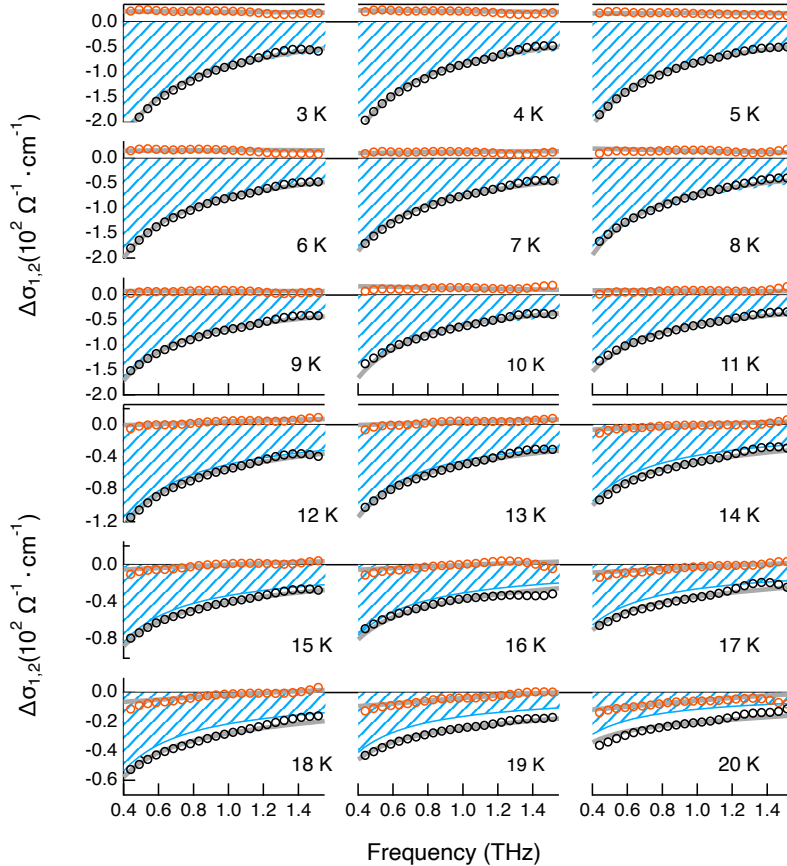


Figure 2. Temperature dependence of the photoinduced THz conductivity change. Real ($\Delta\sigma_1$, orange circles) and imaginary ($\Delta\sigma_2$, black circles) parts of the photoinduced change of the complex conductivities at various temperatures measured at a fixed delay of $\Delta t = 50$ ps. The grey curves represent the fitting model. The shading pattern represents contribution from $\Delta\rho_s$.

To explore the temperature dependence of the superfluid density and pairing dynamics, we measured $\Delta\tilde{\sigma}$ at different temperatures. The data recorded at a fixed delay of 50 ps are displayed in Fig. 2. Under identical pumping conditions, the magnitude of both $\Delta\sigma_1$ and $\Delta\sigma_2$ decreases monotonically with increasing temperature, indicating a gradual reduction in $\Delta\rho_s$ and $\Delta\rho_n$. At temperatures well below T_c , the positive $\Delta\sigma_1$ and the negative $\Delta\sigma_2$ with its characteristic $1/\omega$ superfluid response are well described by the two fluid model. As the temperature approaches T_c , however, $\Delta\sigma_1$ partially crosses zero and eventually becomes fully negative, whereas $\Delta\sigma_2$ remains negative. This phenomenon is not fully captured by the two-fluid model, which has been attributed to the fluctuating superconductivity near T_c .[13]

The two-fluid model assumes that $\Delta\tilde{\sigma}$ arises solely from Cooper pair breaking, with the Drude component originating only from the photogenerated quasiparticles, while thermal quasiparticles remain unaffected. However, as proposed by Cheng and co-workers,[13] optical excitation may also promote a small fraction of the thermal quasiparticles into a nonequilibrium state (i.e., “hot” quasiparticles). This would reduce the thermal quasiparticle conductivity (i.e., decrease the normal conductivity), thereby offsetting the positive contribution to $\Delta\sigma_1$. By accounting for this photoinduced perturbation of the Drude conductivity from the thermal quasiparticle excitation, the behavior of $\Delta\tilde{\sigma}$ near T_c can be well reproduced. Fits based on this extended two-fluid model (see Eq. S2 in the SI) reveal that, in contrast to $\Delta\sigma_1$, the Drude contribution to $\Delta\sigma_2$ from thermal quasiparticle excitation is negligible at temperatures well below

T_c , where the response is dominated by $\Delta\rho_s$ (shading pattern, Fig. 2a). Near T_c , however, the clear deviation between the measured $\Delta\sigma_2$ and the contribution from $\Delta\rho_s$ indicates an appreciable effect from thermal quasiparticle excitation. Finally, we find that $\Delta\tilde{\sigma}$ at other delays exhibits a similar temperature dependence (Figs. S3-S5), all of which is well described by the same extended model.

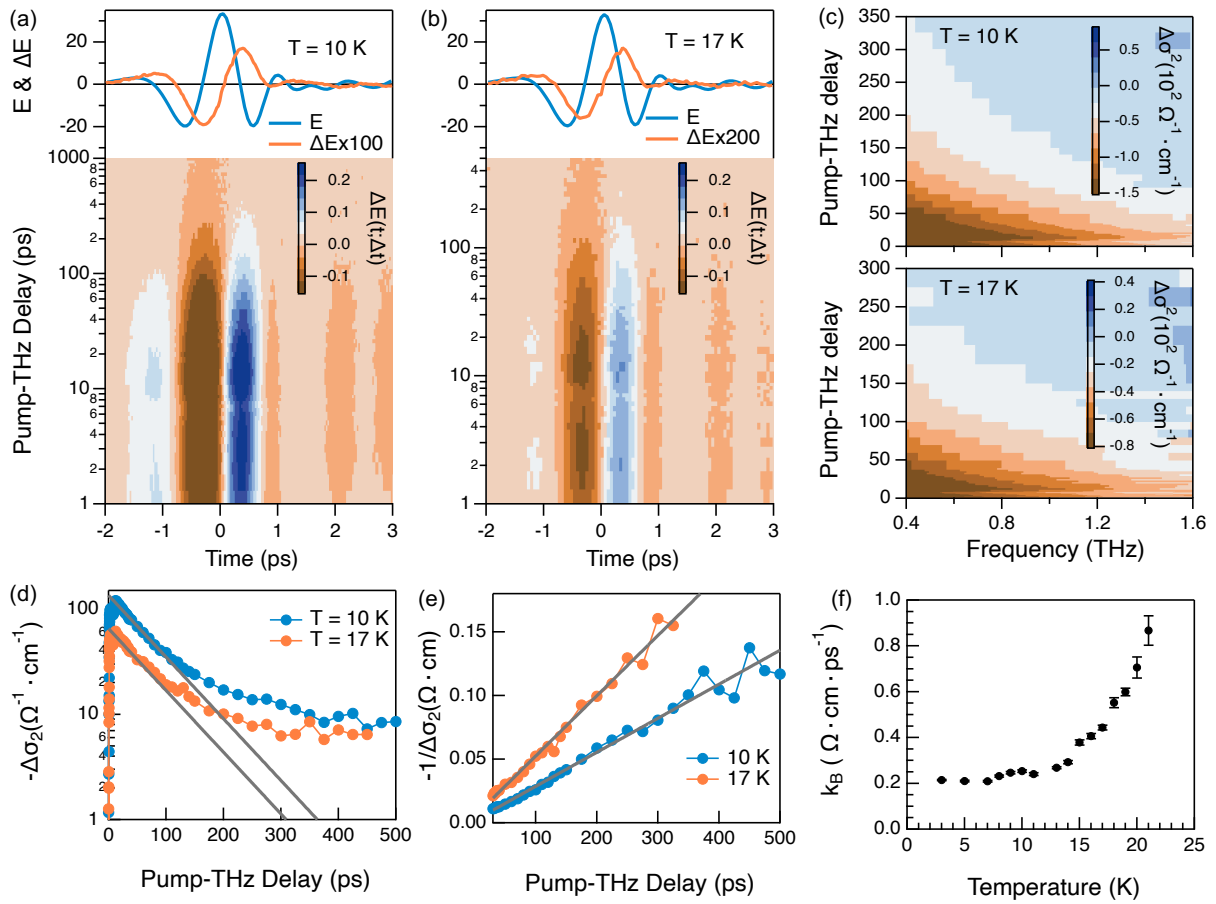


Figure 3. Temperature dependence of the superfluid recovery dynamics. (a)-(b) Time resolved THz waveforms measured at two different temperatures. The orange and cyan curves in top panels represent $\Delta E(t; \Delta t)$ and $E(t)$, respectively. (c) Time resolved $\Delta\sigma_2$ extracted from panel (a) and (b). (d) Kinetics of $\Delta\sigma_2$ at 1 THz at indicated temperatures. (e) The reciprocal of the $\Delta\sigma_2$ kinetics at indicated temperatures. (f) Temperature dependence of the bimolecular recombination rate constant of the photogenerated quasiparticles.

The temporal evolution of THz waveforms at two representative temperatures shows a progressive decay in amplitude with negligible phase shift as Δt increases (Fig. 3a-b), from which $\Delta\tilde{\sigma}$ at various Δt can be extracted. The resulting temporal evolution of $\Delta\sigma_2$ (Fig. 3c) reveals a long-lived feature of the superfluid depletion that persists for several hundred picoseconds. This slow recovery of the superfluid density has previously been attributed to a bottleneck effect caused by the presence of superconducting gap.[23,24] According to the Rothwarf-Taylor (RT) model, superfluid recovery proceeds via the recombination of photogenerated quasiparticles into Cooper pairs. This recombination can occur primarily through two pathways: bimolecular recombination between two photogenerated quasiparticles, or between a photogenerated and a thermal quasiparticle.[18,25-28] The former gives rise to a bimolecular recovery, whereas the latter leads to a single-exponential recovery. If a quasi-equilibrium state is established between the quasiparticles and nonthermal phonons due to the strong electron-phonon coupling, the superfluid recovery dynamics become governed by the decay of this quasi-equilibrium state, typically limited by the nonthermal phonon lifetime, which potentially masks the quasiparticle recombination dynamics.[20,28,29]

Since $\Delta\sigma_2$ is dominated by $\Delta\rho_s$, its kinetics serve as a direct probe of the superfluid recovery dynamics. The kinetic traces at representative temperatures exhibit a strongly nonexponential decay, as evident from Fig. 3d, where y-axis is plotted on a logarithmic scale. The reciprocals of $\Delta\sigma_2$ kinetics increase linearly with Δt (Fig. 3e), a hallmark of a bimolecular recombination process. This suggests that the recovery is governed by the mutual recombination between photogenerated quasiparticles, a phenomenon previously observed in cuprate superconductors.[18,26] The $\Delta\sigma_2$ kinetics at all other measured temperatures also conform to this bimolecular pattern (Fig. S6). The bimolecular recombination rate constant (k_B), extracted from

the kinetics fitting, is nearly temperature-independent for $T < 15$ K but rises steeply above 15 K. This temperature trend contrasts with observations in cuprates, where k_B depends weakly on temperature,[26] likely because the participation of thermal quasiparticles at elevated temperatures causes the quasiparticle recombination in cuprates to significantly deviates from a pure bimolecular mechanism.[18] A systematic study will be needed to resolve this discrepancy.

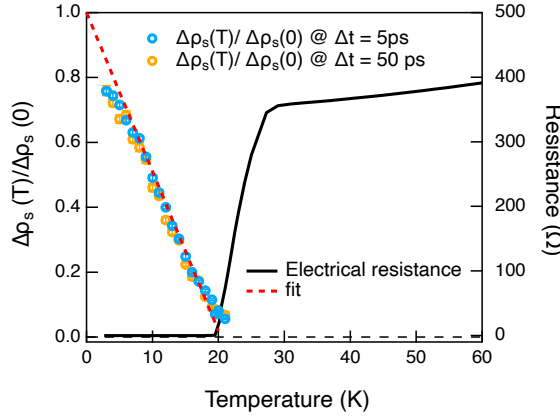


Figure 4. Temperature-dependent superfluid density. The cyan and orange circles represent the temperature-dependent $\Delta\rho_s(T)/\Delta\rho_s(0)$ at fixed pump-THz delay of 5 ps and 50 ps, respectively. The lines are the linear fits. The black curve is the temperature-dependent resistance.

The recovery of $\Delta E(t; \Delta t)$ is relatively slow below T_c (Fig. 3d), which is also evidenced by the small difference between $\Delta\rho_s$ recorded at 5 ps and 50 ps for different temperatures (Fig. S7). This slow recovery justifies using $\Delta\rho_s$ obtained from fitting $\Delta\tilde{\sigma}(\omega)$ at a short delay (e.g., $\Delta t = 5$ ps) as a close approximation to the initial density of broken Cooper pairs. It has been previously established that the photo-destroyed superfluid density is proportional to the equilibrium superfluid density (i.e., $\Delta\rho_s \propto \rho_s$),[18,23] implying that $\Delta\rho_s$ and ρ_s should share the same temperature dependence. $\Delta\rho_s$ probed at short delays exhibit a linear dependence on temperature (Fig. 4 and Fig.

S7). This linear dependence is a hallmark of the $d_{x^2-y^2}$ wave pairing in the clean limit, widely observed in high-quality cuprate superconductors,[30-37] and is described by the relation,[38,39]

$$\frac{\Delta\rho_s(T)}{\Delta\rho_s(0)} = \frac{\rho_s(T)}{\rho_s(0)} = \left[1 - \frac{2\ln 2}{\Delta(0)}k_B T\right] \quad (2)$$

where $\Delta(0)$ is the superconducting gap magnitude at zero temperature. The wide range of linear temperature dependence, extending from near T_c (~ 18 K) down to 5 K, is consistent with observations in cuprates.[35,36] Below 5 K, the data begin to deviate from the linear trend, reminiscent of the crossover to a quadratic behavior in $\rho_s(T)$ that occurs in cuprates at low temperature regime.[35-37] Thus, the superconducting gap structure in this nickelate sample should be analogous to that in clean d-wave cuprate superconductors. In contrast, a quadratic temperature dependence of $\rho_s(T)$ has recently been reported in lanthanum- and praseodymium-based nickelate superconductors with $T_c \leq 10$ K, which is a signature of d-wave pairing in the dirty limit.[11,12]

The linear fit of $\Delta\rho_s(T)/\Delta\rho_s(0)$ based on Eq. 2 (Fig. 4) yields $\Delta(0) = 2.5 \pm 0.1$ meV, giving a ratio $2\Delta(0)/k_B T_c \approx 3$. This gap-to- T_c , consistent with the value reported for Sr-doped neodymium nickelate film,[13] suggests that the measured nickelate film lies in the weak-coupling regime. The impurity influence on superconducting behaviors is often assessed by the ratio of the mean free path to the coherence length, $l/\xi = \pi\Delta(0)/\hbar\tau_0^{-1}$, where τ_0^{-1} is the scattering rate for the equilibrium quasiparticles. Fitting $\Delta\tilde{\sigma}(\omega)$ with the extended two-fluid model yields $\tau_0^{-1} = 8.3$ THz, slightly higher than the value reported for the Sr-doped neodymium nickelate film.[13] Substituting τ_0^{-1} and $\Delta(0)$ into the expression above gives $l/\xi \sim 1.5$, confirming that the film is in the clean limit. This result is compatible with the observed linear temperature dependence of $\Delta\rho_s$.

In summary, we have investigated the pairing mechanism of infinite-layer samarium nickelate superconductors using ultrafast optical pump-THz probe spectroscopy. Temperature dependent measurements provide evidence for d-wave pairing symmetry in the clean limit, closely mirroring the behavior in cuprate superconductors.

Acknowledgements

This work was supported by the Key Research Program of the State Key Laboratory of Cryogenic Science and Technology (T-2025cryo-18), National Natural Science Foundation of China (22473093, 52525208 and 12274061), the National Key Research and Development Program of China (2023YFA1406301), Science and Technology Department of Sichuan Province (2024ZYD0164), and the Fundamental Research Funds for the Central Universities (20720240150).

Reference:

- [1] D. Li, K. Lee, B. Y. Wang, M. Osada, S. Crossley, H. R. Lee, Y. Cui, Y. Hikita, and H. Y. Hwang, Superconductivity in an infinite-layer nickelate, *Nature* **572**, 624 (2019).
- [2] H. Sakakibara, H. Usui, K. Suzuki, T. Kotani, H. Aoki, and K. Kuroki, Model Construction and a Possibility of Cupratelike Pairing in a New d9 Nickelate Superconductor (Nd,Sr)NiO₂, *Phys. Rev. Lett.* **125**, 077003 (2020).
- [3] F. Lechermann, Multiorbital Processes Rule the Nd_{1-x}Sr_xNiO₂ Normal State, *Phys. Rev. X* **10**, 041002 (2020).
- [4] X. Wu, D. Di Sante, T. Schwemmer, W. Hanke, H. Y. Hwang, S. Raghu, and R. Thomale, Robust dx₂-y₂-wave superconductivity of infinite-layer nickelates, *Phys. Rev. B* **101**, 060504 (2020).
- [5] M. Kitatani, L. Si, O. Janson, R. Arita, Z. Zhong, and K. Held, Nickelate superconductors—a renaissance of the one-band Hubbard model, *NPJ Quantum Mater.* **5**, 59 (2020).
- [6] P. Werner and S. Hoshino, Nickelate superconductors: Multiorbital nature and spin freezing, *Phys. Rev. B* **101**, 041104 (2020).
- [7] Y. Nomura, M. Hirayama, T. Tadano, Y. Yoshimoto, K. Nakamura, and R. Arita, Formation of a two-dimensional single-component correlated electron system and band engineering in the nickelate superconductor NdNiO₂, *Phys. Rev. B* **100**, 205138 (2019).
- [8] Z. Wang, G.-M. Zhang, Y.-f. Yang, and F.-C. Zhang, Distinct pairing symmetries of superconductivity in infinite-layer nickelates, *Phys. Rev. B* **102**, 220501 (2020).

[9] Z. Li and S. G. Louie, Two-Gap Superconductivity and the Decisive Role of Rare-Earth d Electrons in Infinite-Layer Nickelates, *Phys. Rev. Lett.* **133**, 126401 (2024).

[10] Q. Gu, Y. Li, S. Wan, H. Li, W. Guo, H. Yang, Q. Li, X. Zhu, X. Pan, Y. Nie, and H.-H. Wen, Single particle tunneling spectrum of superconducting $\text{Nd}_{1-x}\text{Sr}_x\text{NiO}_2$ thin films, *Nat. Commun.* **11**, 6027 (2020).

[11] S. P. Harvey, B. Y. Wang, J. Fowlie, M. Osada, K. Lee, Y. Lee, D. Li, and H. Y. Hwang, Evidence for nodal superconductivity in infinite-layer nickelates, *Proc. Natl Acad. Sci. USA* **122**, e2427243122 (2025).

[12] L. E. Chow, S. Kunniniyil Sudheesh, Z. Y. Luo, P. Nandi, T. Heil, J. Deuschle, S. W. Zeng, Z. T. Zhang, S. Prakash, X. M. Du, Z. S. Lim, P. A. van Aken, E. E. M. Chia, and A. Ariando, 2022), p. arXiv:2201.10038.

[13] B. Cheng, D. Cheng, K. Lee, L. Luo, Z. Chen, Y. Lee, B. Y. Wang, M. Mootz, I. E. Perakis, Z.-X. Shen, H. Y. Hwang, and J. Wang, Evidence for d-wave superconductivity of infinite-layer nickelates from low-energy electrodynamics, *Nat. Mater.* **23**, 775 (2024).

[14] Q. Gu and H.-H. Wen, Superconductivity in nickel-based 112 systems, *The Innovation* **3**, 100202 (2022).

[15] B. Y. Wang, K. Lee, and B. H. Goodge, Experimental Progress in Superconducting Nickelates, *Annu. Rev. Condens. Matter Phys.* **15**, 305 (2024).

[16] S. L. E. Chow, Z. Luo, and A. Ariando, Bulk superconductivity near 40 K in hole-doped SmNiO_2 at ambient pressure, *Nature* **642**, 58 (2025).

[17] M. Yang, H. Wang, J. Tang, J. Luo, X. Wu, R. Mao, W. Xu, G. Zhou, Z. Dong, and B. Feng, Enhanced superconductivity in co-doped infinite-layer samarium nickelate thin films, arXiv preprint arXiv:2503.18346 (2025).

[18] R. A. Kaindl, M. A. Carnahan, D. S. Chemla, S. Oh, and J. N. Eckstein, Dynamics of Cooper pair formation in $\text{Bi}_2\text{Sr}_2\text{Ca}\text{Cu}_2\text{O}_{8+\delta}$, *Phys. Rev. B* **72**, 060510 (2005).

[19] X. Ding, C. C. Tam, X. Sui, Y. Zhao, M. Xu, J. Choi *et al.*, Critical role of hydrogen for superconductivity in nickelates, *Nature* **615**, 50 (2023).

[20] R. D. Averitt, G. Rodriguez, A. I. Lobad, J. L. W. Siders, S. A. Trugman, and A. J. Taylor, Nonequilibrium superconductivity and quasiparticle dynamics in $\text{YBa}_2\text{Cu}_3\text{O}_{7-\delta}$, *Phys. Rev. B* **63**, 140502 (2001).

[21] S. J. Zhang, Z. X. Wang, H. Xiang, X. Yao, Q. M. Liu, L. Y. Shi, T. Lin, T. Dong, D. Wu, and N. L. Wang, Photoinduced Nonequilibrium Response in Underdoped $\text{YBa}_2\text{Cu}_3\text{O}_{6+x}$ Probed by Time-Resolved Terahertz Spectroscopy, *Phys. Rev. X* **10**, 011056 (2020).

[22] C. Giannetti, M. Capone, D. Fausti, M. Fabrizio, F. Parmigiani, and D. Mihailovic, Ultrafast optical spectroscopy of strongly correlated materials and high-temperature superconductors: a non-equilibrium approach, *Adv. Phys.* **65**, 58 (2016).

[23] J. Demsar, B. Podobnik, V. V. Kabanov, T. Wolf, and D. Mihailovic, Superconducting Gap Δ_c , the Pseudogap Δ_p , and Pair Fluctuations above T_c in Overdoped $\text{Y}_{1-x}\text{Ca}_x\text{Ba}_2\text{Cu}_3\text{O}_{7-\delta}$ from Femtosecond Time-Domain Spectroscopy, *Phys. Rev. Lett.* **82**, 4918 (1999).

[24] V. V. Kabanov, J. Demsar, B. Podobnik, and D. Mihailovic, Quasiparticle relaxation dynamics in superconductors with different gap structures: Theory and experiments on $\text{YBa}_2\text{Cu}_3\text{O}_{7-\delta}$, *Phys. Rev. B* **59**, 1497 (1999).

[25] J. Demsar, R. D. Averitt, A. J. Taylor, V. V. Kabanov, W. N. Kang, H. J. Kim, E. M. Choi, and S. I. Lee, Pair-Breaking and Superconducting State Recovery Dynamics in MgB₂, *Phys. Rev. Lett.* **91**, 267002 (2003).

[26] N. Gedik, P. Blake, R. C. Spitzer, J. Orenstein, R. Liang, D. A. Bonn, and W. N. Hardy, Single-quasiparticle stability and quasiparticle-pair decay in YBa₂Cu₃O_{6.5}, *Phys. Rev. B* **70**, 014504 (2004).

[27] I. M. Vishik, F. Mahmood, Z. Alpichshev, N. Gedik, J. Higgins, and R. L. Greene, Ultrafast dynamics in the presence of antiferromagnetic correlations in electron-doped cuprate La_{2-x}Ce_xCuO_{4±δ}, *Phys. Rev. B* **95**, 115125 (2017).

[28] V. V. Kabanov, J. Demsar, and D. Mihailovic, Kinetics of a Superconductor Excited with a Femtosecond Optical Pulse, *Phys. Rev. Lett.* **95**, 147002 (2005).

[29] G. P. Segre, N. Gedik, J. Orenstein, D. A. Bonn, R. Liang, and W. N. Hardy, Photoinduced Changes of Reflectivity in Single Crystals of YBa₂Cu₃O_{6.5} (Ortho II), *Phys. Rev. Lett.* **88**, 137001 (2002).

[30] W. N. Hardy, D. A. Bonn, D. C. Morgan, R. Liang, and K. Zhang, Precision measurements of the temperature dependence of λ in Ba₂Cu₃O_{6.95}: Strong evidence for nodes in the gap function, *Phys. Rev. Lett.* **70**, 3999 (1993).

[31] T. Jacobs, S. Sridhar, Q. Li, G. D. Gu, and N. Koshizuka, In-Plane and c-Axis Microwave Penetration Depth of Bi₂Sr₂Ca₁Cu₂O_{8+δ} Crystals, *Phys. Rev. Lett.* **75**, 4516 (1995).

[32] S.-F. Lee, D. C. Morgan, R. J. Ormeno, D. M. Broun, R. A. Doyle, J. R. Waldram, and K. Kadowaki, a-b Plane Microwave Surface Impedance of a High-Quality Bi₂Sr₂CaCu₂O₈ Single Crystal, *Phys. Rev. Lett.* **77**, 735 (1996).

[33] D. M. Broun, D. C. Morgan, R. J. Ormeno, S. F. Lee, A. W. Tyler, A. P. Mackenzie, and J. R. Waldram, In-plane microwave conductivity of the single-layer cuprate Tl₂Ba₂CuO_{6+δ}, *Phys. Rev. B* **56**, R11443 (1997).

[34] C. Panagopoulos, J. R. Cooper, G. B. Peacock, I. Gameson, P. P. Edwards, W. Schmidbauer, and J. W. Hodby, Anisotropic magnetic penetration depth of grain-aligned HgBa₂Ca₂Cu₃O_{8+δ}, *Phys. Rev. B* **53**, R2999 (1996).

[35] N. R. Lee-Hone, J. S. Dodge, and D. M. Broun, Disorder and superfluid density in overdoped cuprate superconductors, *Phys. Rev. B* **96**, 024501 (2017).

[36] D. M. Broun, W. A. Hutmama, P. J. Turner, S. Özcan, B. Morgan, R. Liang, W. N. Hardy, and D. A. Bonn, Superfluid Density in a Highly Underdoped YBa₂Cu₃O_{6+y} Superconductor, *Phys. Rev. Lett.* **99**, 237003 (2007).

[37] I. Božović, X. He, J. Wu, and A. T. Bollinger, Dependence of the critical temperature in overdoped copper oxides on superfluid density, *Nature* **536**, 309 (2016).

[38] R. Prozorov and R. W. Giannetta, Magnetic penetration depth in unconventional superconductors, *Supercond. Sci. Technol.* **19**, R41 (2006).

[39] C. Panagopoulos and T. Xiang, Relationship between the Superconducting Energy Gap and the Critical Temperature in High-T_c Superconductors, *Phys. Rev. Lett.* **81**, 2336 (1998).